

Supporting Information

Lanthanide Electronic Perturbation in Pt-Ln (La, Ce, Pr and Nd) alloys for Enhanced Methanol Oxidation Reaction Activity

Shuai Zhang,^a Zhichao Zeng,^a Qingqing Li,^a Bolong Huang,^{b*} Xinyu Zhang,^c Yaping Du^{a*} and Chun-Hua Yan^{a,d,e}

Experimental Section/Methods

Chemicals. $\text{H}_2\text{PtCl}_6 \cdot 6\text{H}_2\text{O}$ (99.95%, Alfa), Nafion solution (5 wt.%, Alfa), CN_2H_2 (99%, Sigma-Aldrich), 10% H_2/Ar mixing gas ($\geq 99.999\%$, $\text{H}_2\text{O} \leq 3$ ppm, $\text{O}_2 \leq 2$ ppm, Air Liquide), $\text{LaCl}_3 \cdot 7\text{H}_2\text{O}$ (99.99%, Aladdin), $\text{CeCl}_3 \cdot 7\text{H}_2\text{O}$ (99.99%, Aladdin), $\text{PrCl}_3 \cdot 6\text{H}_2\text{O}$ (99.99%, Aladdin), $\text{NdCl}_3 \cdot 6\text{H}_2\text{O}$ (99.99%, Aladdin), CH_3OH ($\geq 99.9\%$, Innochem), KOH (99.999%, Aladdin), carbon (Ketjen Black EC300J, Lion), Milli-Q water (≥ 18.2 $\text{M}\Omega \cdot \text{cm}$). All the chemicals were used without further purification.

Catalyst Synthesis. 0.5 g $\text{H}_2\text{PtCl}_6 \cdot 6\text{H}_2\text{O}$, CN_2H_2 , rare earth chloride (the mole ratio of Pt, Ln and CN_2H_2 was 3: 2: 50) and 0.5 g carbon were mixed in an agate mortar. The obtained mixture was then transferred into a tube furnace for heat-treatment. The purging gas was 10% H_2/Ar with the flow rate maintained at 340 mL min^{-1} throughout the heat-treatment. The furnace temperature was first raised from room temperature to $150 \text{ }^\circ\text{C}$ at the rate of $10 \text{ }^\circ\text{C min}^{-1}$. The temperature was maintained at $150 \text{ }^\circ\text{C}$ for 30 min, then increased to $650 \text{ }^\circ\text{C}$ at the rate of $5 \text{ }^\circ\text{C min}^{-1}$. It was kept at this temperature for 2 h, and at last cooled down to room temperature. The obtained product was leached in 500 mL of 0.5 M H_2SO_4 at $60 \text{ }^\circ\text{C}$ for 1 h under continuous stirring. The product was then thoroughly washed with Milli-Q water, and vacuum-dried at $80 \text{ }^\circ\text{C}$ for 6 h, yielding the final catalyst.

Electrochemical measurements. The 1 mg synthesized catalysts were dispersed in a mixture of 495 μL ultrapure water, 495 μL isopropanol, and 10 μL Nafion solution, after sonication for 1 h. Electrochemical measurements were conducted on a CHI 660E Electrochemical Workstation (Shanghai Chenhua Instrument Corporation, China) in a conventional three-electrode cell. The graphite rod electrode as the counter electrode and a saturated calomel electrode (SCE) as the reference electrode. The working electrode was a glassy carbon electrode (GCE, diameter: 5 mm, area: 0.196 cm^2). five microliters of the catalyst were dropped onto the GCE surface for

further electrochemical tests. All the potentials reported in this work were converted to the reversible hydrogen electrode (RHE). The mass activity and specific activity were normalized by the mass of Pt metal (determined by the ICP tests) and electrochemically active surface area (ECSA) of catalysts (determined by integrating the Pt reduction peak in CV). For MOR stability test, the accelerated degradation test was conducted by continuous cycling between 0.1 and 1.2 V at the scan rate of 50 mV s⁻¹ in 1.0 M KOH and 1.0 M ethanol. The chronoamperometry measurements were conducted at 0.65 V in the same solution. For the CO stripping tests, the CO oxidation experiments were carried out in 0.1 m KOH solution. Before the test, the solution was purged with argon for 30 min, and then bubbled with CO gas (99.9%) for 15 min to achieve the maximum coverage of CO at the Pt active centres. The residual CO in the solution was excluded by argon for 30 min. Electrochemical impedance spectroscopy (EIS) measurements were measured at 0.6 V vs. RHE in the frequency range from 50 kHz to 0.01 Hz in Ar saturated solution.

Physical characterization. The powder X-ray diffraction (XRD) measurements were carried out on Rigaku Smart Lab 3kW, X-ray diffraction diffractometer using monochromatized Cu K α radiation ($\lambda=1.5418$ Å). X-ray photoelectron spectra (XPS) were conducted using a Thermo Scientific ESCALAB 250Xi instrument equipped with an Al X-ray excitation source. High-angle annular dark-field scanning transmission electron microscopy (HAADF-STEM) images were obtained at 300 kV with a FEI Titan Cubed Themis G2 300. High-resolution transmission electron microscopy (HRTEM) images were obtained using a Field-emission transmission electron microscope (JEM-2800, Japan). The contents of the electrocatalyst were analyzed by Inductively Coupled Plasma Mass Spectrometry (Elan drc-e, USA). The surface areas of the samples were measured using the Brunauer–Emmett–Teller (BET) method with the equipment of Micrometrics (JW–BK112 system).

Calculation Setup. DFT calculations within CASTEP packages have been applied in this work to investigate the MOR on Pt₅Ln.¹ For all the calculations, we choose the generalized gradient approximation (GGA) and Perdew-Burke-Ernzerhof (PBE) to describe the exchange-correlation energy.²⁻⁴ The plane-wave basis cutoff energy has been set to 380 eV based on the ultrafine quality. The ultrasoft pseudopotentials with the Broyden-Fletcher-Goldfarb-Shannon (BFGS) algorithm have been utilized for all the geometry optimizations. To achieve the balance between computation cost and accuracy, the coarse quality of the k-point set is used for the energy minimizations.⁵ According to the experimental characterizations, the Pt₅Ln structures have been cleaved from the (002) surface of Pt₅Ln with six-layer thickness. To guarantee full relaxations for all the structure and adsorption of intermediates, we have applied 20 Å vacuum space in the z-axis for sufficient space. Meanwhile, the convergence criteria of the geometry optimizations have been set as follows: the Hellmann-Feynman forces on the atom should be less than 0.001 eV/Å; the total energy difference and the inter-ionic displacement should be less than 5×10^{-5} eV/atom and 0.005 Å, respectively.

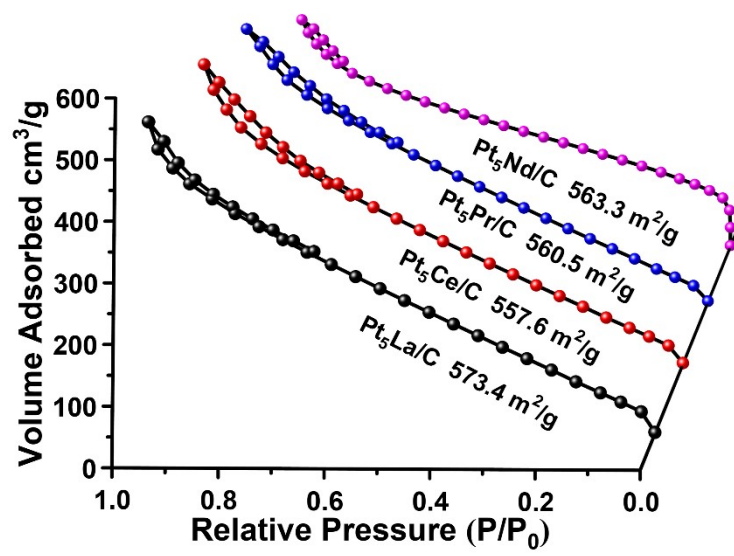


Figure S1. N₂ adsorption and desorption isotherms of Pt₅La/C, Pt₅Ce/C, Pt₅Pr/C, Pt₅Nd/C samples.

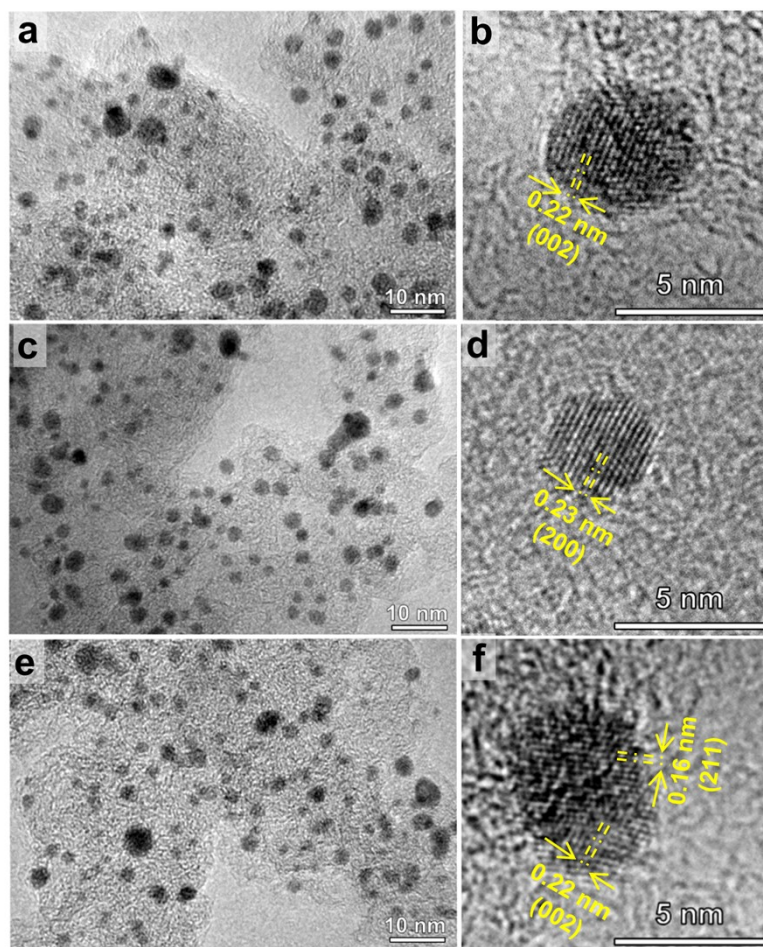


Figure S2. TEM and HRTEM images of Pt₅La/C, Pt₅Pr/C and Pt₅Nd/C samples. (a) TEM image of Pt₅La/C. (b) HRTEM image of Pt₅La/C. (c) TEM image of Pt₅Pr/C. (d) HRTEM image of Pt₅Pr/C. (e) TEM image of Pt₅Nd/C. (f) HRTEM image of Pt₅Nd/C.

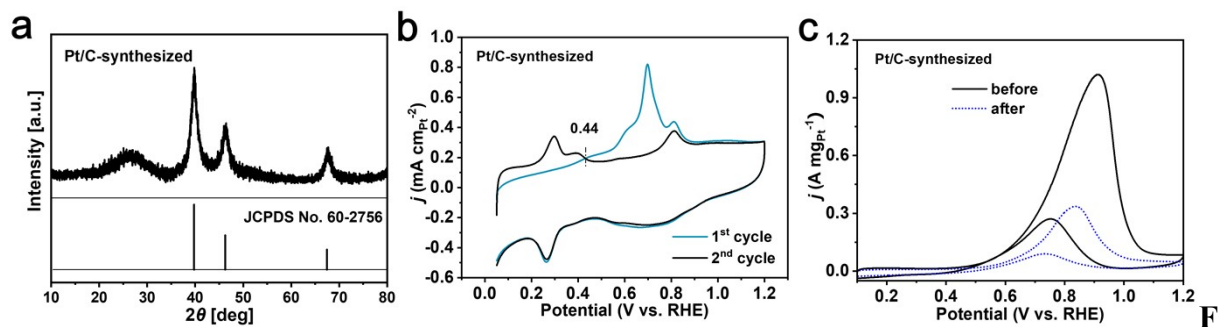


figure S3. (a) XRD patterns of synthesized Pt/C, (b) CO-stripping voltammetry of synthesized Pt/C, (c) synthesized Pt/C samples before and after 1000 cycles.

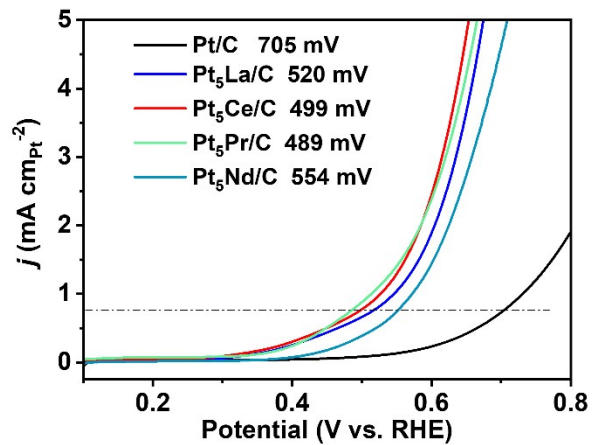


Figure S4. The onset potential (the specific activity of $0.78 \text{ mA cm}^{-2}_{\text{Pt}}$) of Pt₅La/C, Pt₅Ce/C/C, Pt₅Pr/C, Pt₅Nd/C samples and commercial Pt/C.

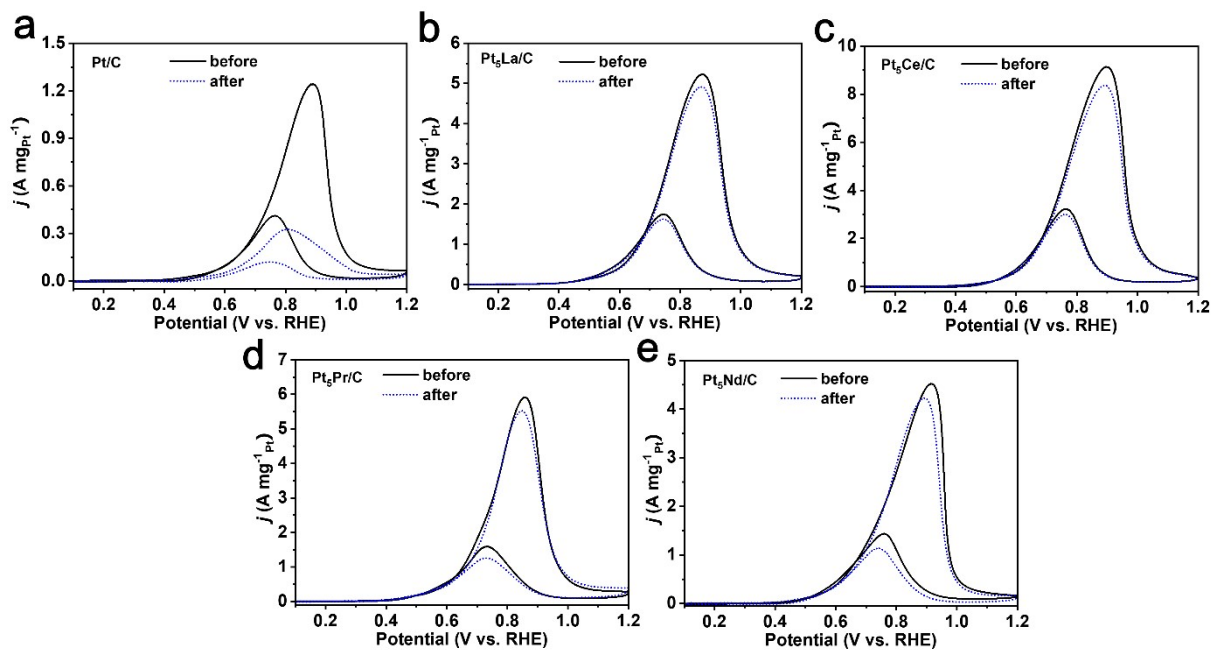


Figure S5. Electrocatalytic performance tests. CV curves of (a) commercial Pt/C, (b) Pt₅La/C, (c) Pt₅Ce/C, (d) Pt₅Pr/C and (e) Pt₅Nd samples before and after 1000 cycles.

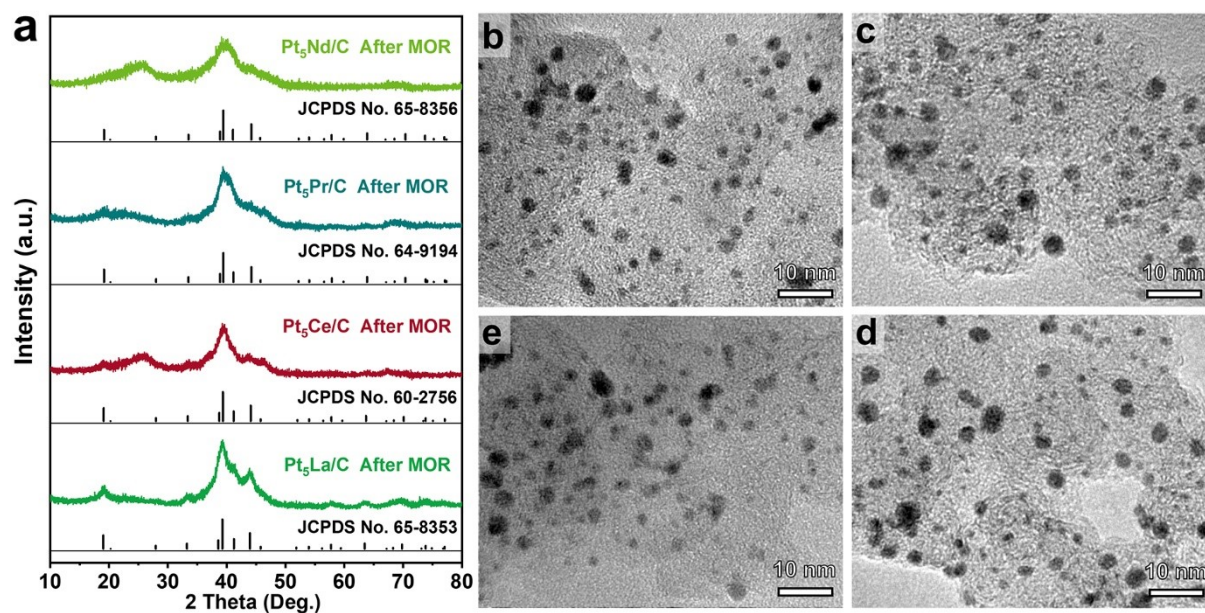


Figure S6. XRD patterns and TEM images after stability test for MOR. (a) XRD patterns of Pt₅La/C, Pt₅Ce/C, Pt₅Pr/C, Pt₅Nd/C samples after 1000 cycles test for MOR. The TEM images of (b) Pt₅La/C, (c) Pt₅Ce/C, (d) Pt₅Pr/C and (e) Pt₅Nd samples after 1000 cycles test for MOR.

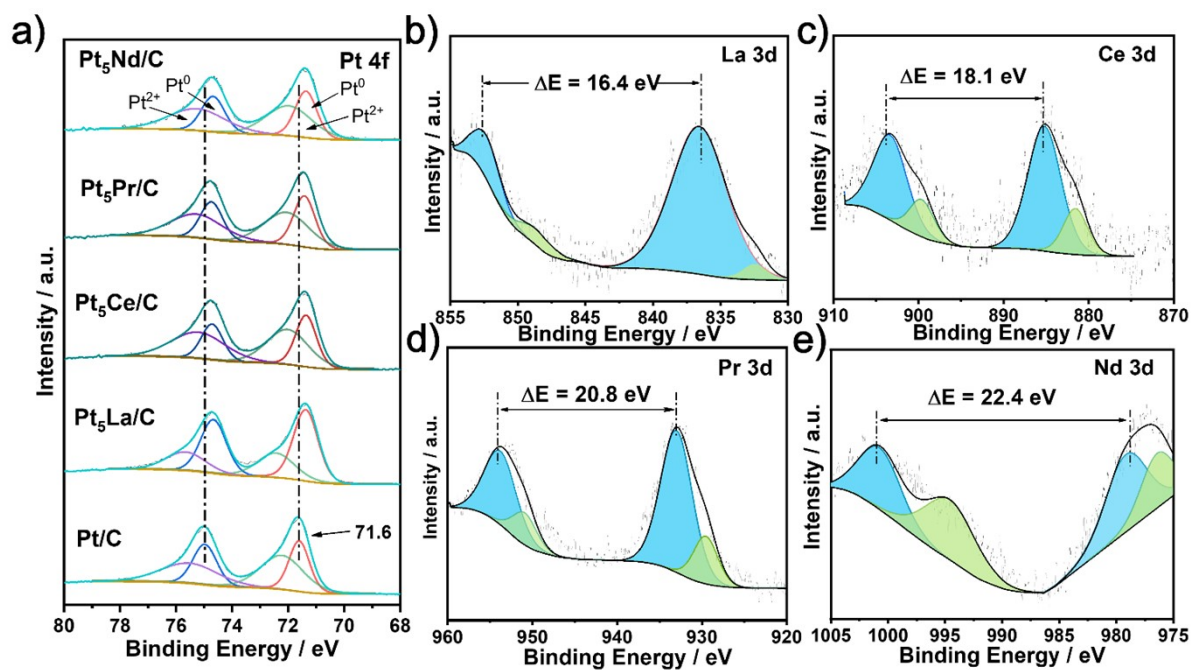


Figure S7. High resolution XPS spectra after MOR test. (a) Pt 4f of Pt₅La/C, Pt₅Ce/C, Pt₅Pr/C, Pt₅Nd/C samples and commercial Pt/C. (b) La 3d of Pt₅La/C. (c) Ce 3d of Pt₅Ce/C. (d) Pr 3d of Pt₅Pr/C, (e) Nd 3d of Pt₅Nd/C.

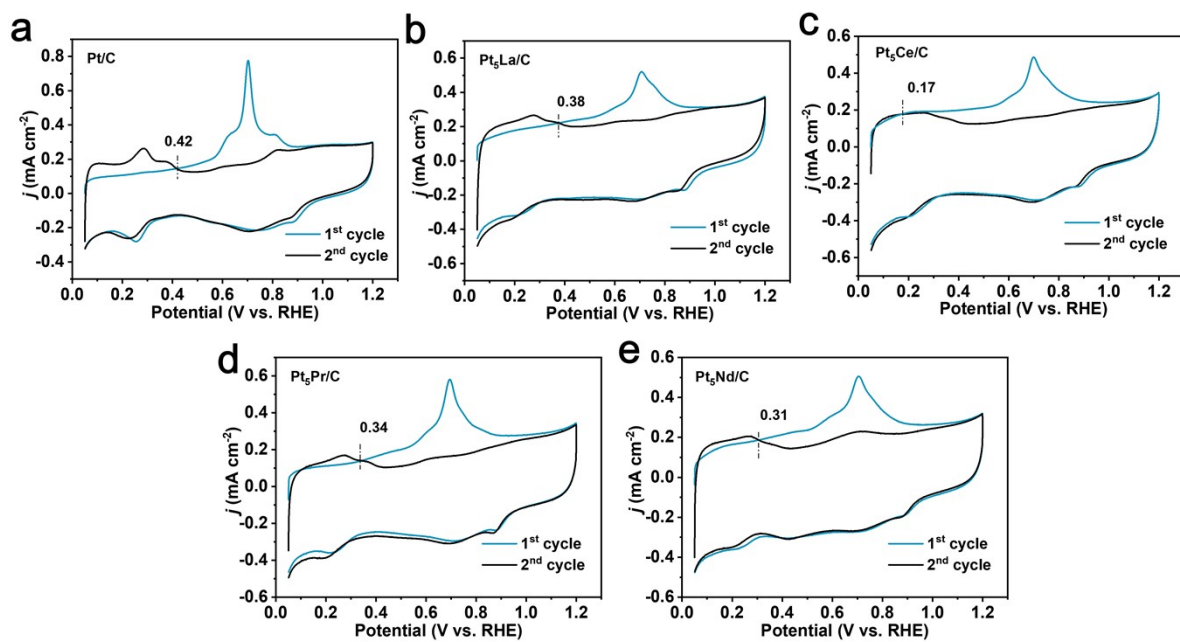


Figure S8. CO-stripping voltammetry of (a) commercial Pt/C, (b) Pt₅La/C, (c) Pt₅Ce/C, (d) Pt₅Pr/C and (e) Pt₅Nd samples.

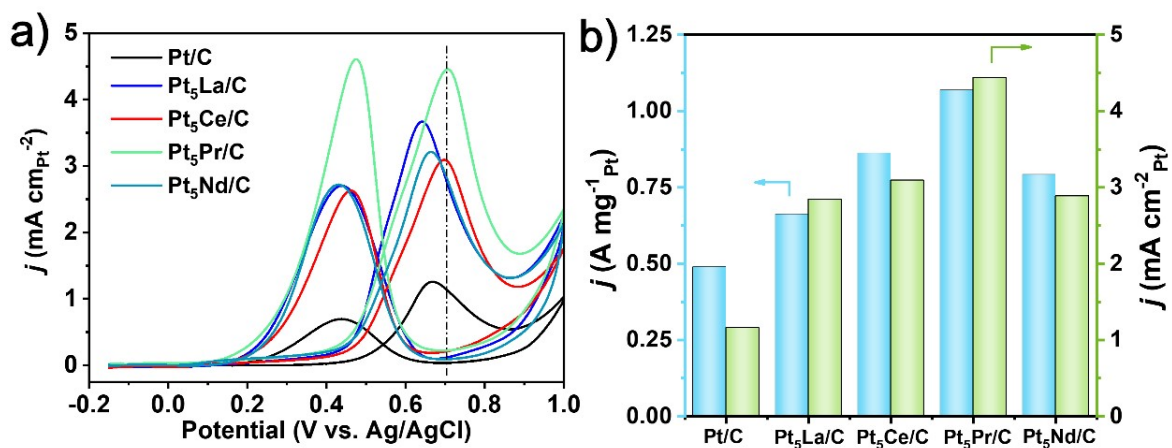


Figure S9. Methanol electro-oxidation performance of Pt₅La/C, Pt₅Ce/C, Pt₅Pr/C, Pt₅Nd/C samples and commercial Pt/C in 0.5 M H₂SO₄ + 1 M CH₃OH electrolyte. (a) CV curves. (b) Peak values of mass activity and area activity.

Table S1.

The ICP data of Pt₅La/C, Pt₅Ce/C, Pt₅Pr/C, Pt₅Nd/C samples.

Sample	Pt/wt%	La/wt%	Ce/wt%	Pr/wt%	Nd/wt%	Stoichiometry
Pt ₅ La/C	15.38	1.59	-	-	-	Pt _{87.3} La _{12.7}
Pt ₅ Ce/C	14.87	-	2.00	-	-	Pt _{84.2} Ce _{15.8}
Pt ₅ Pr/C	15.31	-	-	1.99	-	Pt _{84.7} Pr _{15.3}
Pt ₅ Nd/C	15.29	-	-	-	1.54	Pt _{88.1} Nd _{11.9}

Table S2.

Solution resistance (R_s) and charge transfer resistance (R_{ct}) of Pt₅La/C, Pt₅Ce/C, Pt₅Pr/C, Pt₅Nd/C samples and commercial Pt/C in 1 M KOH + 1 M CH₃OH electrolyte at 0.6 V vs. RHE.

	R_s/Ω	R_{ct}/Ω
Pt/C	9.356	1252.0
Pt ₅ La/C	10.08	386.8
Pt ₅ Ce/C	11.57	108.1
Pt ₅ Pr/C	11.82	257.5
Pt ₅ Nd/C	11.84	543.6

Table S3.

Comparing the catalytic performance of Pt₅La/C, Pt₅Ce/C, Pt₅Pr/C, Pt₅Nd/C samples with the ever-reported alloy MOR catalysts.

Catalysts	Electrolyte	Mass Activity	Specific Activity	References
Pt ₅ La/C		5.23 A mg ⁻¹ Pt	22.41 mA cm ⁻² Pt	
Pt ₅ Ce/C	1 M KOH +1 M MeOH	9.13A mg ⁻¹ Pt	32.74 mA cm ⁻² Pt	This work
Pt ₅ Pr/C		5.91A mg ⁻¹ Pt	24.54 mA cm ⁻² Pt	
Pt ₅ Nd/C		4.52A mg ⁻¹ Pt	16.47 mA cm ⁻² Pt	
PtZn intermetallic NPs	0.1 M KOH +0.5 M MeOH	~0.58 A mg ⁻¹	1.14 mA cm ⁻² Pt	6
Pd ₃ Pb/Pt _{2.37} Pb Nanocubes	1 M KOH +1 M MeOH	8.40 A mg ⁻¹ Pt	13.39 mA cm ⁻² Pt	7
SANi-Pt NWs	1 M KOH +1 M MeOH	7.93 A mg ⁻¹ Pt	7.47 mA cm ⁻² Pt	8
Pt _{0.5} Ag ₁	0.5 M KOH +2 M MeOH	~2.92 A mg ⁻¹ Pt	~7.10 mA cm ⁻² Pt	9
CS-Pt ₅₆ Cu ₂₈ Ni ₁₆	1 M KOH +1 M MeOH	7.00 A mg ⁻¹ Pt	14.00 mA cm ⁻² Pt	10
Popcorn-like PtAu	1 M KOH +1 M MeOH	0.60 A mg ⁻¹ Pt	0.84 mA cm ⁻² Pt	11
Pt ₁ Ni ₁ /C	1 M KOH +1 M MeOH	1.75 A mg ⁻¹ Pt	4.90 mA cm ⁻² Pt	12
Pt _{3.5} Pb nerve nanowires	0.5 M KOH +1 M MeOH	2.84 A mg ⁻¹ Pt	6.51 mA cm ⁻² Pt	13
PtCu nanoframes	0.5 M KOH +1 M MeOH	2.26 A mg ⁻¹ Pt	18.20 mA cm ⁻² Pt	14

References

1. Z. S. J. Clark, M. D. Segall, C. J. Pickard, P. J. Hasnip, M. J. Probert, K. Refson, M. C. Payne. *Zeitschrift Fur Kristallographie*, 2005, **220**, 567-570.
2. J. P. Perdew, K. Burke, M. Ernzerhof, *Phys. Rev. Lett.* 1996, **77**, 3865-3868.
3. P. J. Hasnip, C. J. Pickard, *Comput. Phys. Commun.*, 2006, **174**, 24-29.
4. J. P. Perdew, J. A. Chevary, S. H. Vosko, K. A. Jackson, M. R. Pederson, D. J. Singh, C. Fiolhais, *Phys. Rev. B*, 1992, **46**, 6671-6687.
5. J. D. Head, M. C. Zerner, *Chem. Phys. Lett.*, 1985, **122**, 264-270.
6. Qi, C. Xiao, C. Liu, T. W. Goh, L. Zhou, R. M. Ganesh, Y. Pei, X. Li, L. A. Curtiss, W. Huang, *J. Am. Chem. Soc.* 2017, **139**, 4762-4768.
7. X. Wu, Y. Jiang, Y. Yan, X. Li, S. Luo, J. Huang, J. Li, R. Shen, D. Yang, H. Zhang, *Adv. Sci.* 2019, **6**, 1902249.
8. M. Li, K. Duanmu, C. Wan, T. Cheng, L. Zhang, S. Dai, W. Chen, Z. Zhao, P. Li, H. Fei, Y. Zhu, R. Yu, J. Luo, K. Zang, Z. Lin, M. Ding, J. Huang, H. Sun, J. Guo, X. Pan, W. A. Goddard, P. Sautet, Y. Huang, X. Duan, *Nat. Catal.* 2019, **2**, 495-503.
9. Y. Y. Feng, L. X. Bi, Z. H. Liu, D. S. Kong, Z. Y. Yu, *J. Catal.* 2012, **290**, 18-25.
10. J. Huang, Y. Liu, M. Xu, C. Wan, H. Liu, M. Li, Z. Huang, X. Duan, X. Pan, Y. Huang, *Nano Lett.* 2019, **19**, 5431-5436.
11. J. N. Zheng, S. S. Li, X. Ma, F. Y. Chen, A. J. Wang, J. R. Chen, J. J. Feng, *J. Mater. Chem. A*, 2014, **2**, 8386-8395.
12. S. Lu, H. Li, J. Sun, Z. Zhuang, *Nano Res.* 2018, **11**, 2058-2068.
13. L. Huang, Y. Han, X. Zhang, Y. Fang, S. Dong, *Nanoscale* 2017, **9**, 201-207.
14. Z. Zhang, Z. Luo, B. Chen, C. Wei, J. Zhao, J. Chen, X. Zhang, Z. Lai, Z. Fan, C. Tan, M. Zhao, Q. Lu, B. Li, Y. Zong, C. Yan, G. Wang, Z. J. Xu, H. Zhang, *Adv. Mater.* 2016, **28**, 8712-8717.